
Fusion and Cross-Modal Transfer for Zero-Shot Human Action Recognition

Abhi Kamboj

Department of Electrical and Computer Engineering
University of Illinois
Champaign, IL 61820
akamboj2@illinois.edu

Anh Duy Nguyen

Department of Computer Science
University of Illinois
Champaign, IL 61820
duyan2@illinois.edu

Minh Do

Department of Electrical and Computer Engineering
University of Illinois
Champaign, IL 61820
minhdo@illinois.edu

Abstract

Despite living in a multi-sensory world, most AI models are limited to textual and visual interpretations of human motion and behavior. Inertial measurement units (IMUs) provide a salient signal to understand human motion; however, they are challenging to use due to their uninterpretability and scarcity of their data. We investigate a method to transfer knowledge between visual and inertial modalities using the structure of an informative joint representation space designed for human action recognition (HAR). We apply the resulting Fusion and Cross-modal Transfer (FACT) method to a novel setup, where the model does not have access to labeled IMU data during training and is able to perform HAR with only IMU data during testing. Extensive experiments on a wide range of RGB-IMU datasets demonstrate that FACT significantly outperforms existing methods in zero-shot cross-modal transfer.

1 Introduction

Humans naturally can actuate a motion they have only seen before; however, transferring motion knowledge across sensors for machine learning models is nontrivial. Our interaction with computing has historically been centered around visual and textual modalities, which has provided these models an abundance of data. Thus, deep learning based human action recognition (HAR) systems often collapse 3D motion into related but imprecise modalities such as visual data [16, 31, 20, 36] or language models [28, 37, 33, 26, 9]. However, continuous monitoring by cameras or constant input to text models is impractical, limiting the applicability of these models in real-world scenarios.

Inertial Measurement Units (IMUs), which typically provide 3-axis acceleration and 3-axis gyroscopic information on a wearable device, emerge as strong candidates for understanding human motion in a nonintrusive fashion. Smartwatches, smartphones, earbuds and other wearables have enabled the seamless integration of IMUs into daily life [22]. Unfortunately, IMUs remain underutilized within current machine-learning approaches due to numerous challenges, such as the lack of abundant data and the difficulty in interpreting and labeling the data.

Beyond IMUs, various sensing modalities are gaining popularity in wearables (e.g. surface electrocardiogram, electromyography) and ambient monitoring systems (e.g. wifi signals, millimetwave

Radar). This raises the critical question of how to integrate new sensors with existing ones in the absence of labeled data. One promising solution is leverage a well-documented modality to transfer knowledge to another modality, a process known as cross-modal transfer. Ideally, this source modality would be able to teach the new target modality without any human annotation effort. Existing cross-modal learning techniques assume a semi-supervised or fully supervised setup where there exists some labels for each modality during training. Cross-modal learning has not thoroughly been investigated in a zero shot-setting.

We hypothesize that there exists some inherent latent space that can capture the alignment between multiple sensing modalities for human action recognition. We empirically investigate various methods to construct this space and leverage it to perform zero shot transfer between modalities. Specifically, given labeled data from one sensor and unlabeled data from another, we explore whether an intermediate latent structure can be used to infer human actions from new data obtained solely from the second sensor.

Our method to perform Fusion and Cross-modal Transfer (FACT) through the hidden correlation between modalities, was tested on RGB and IMU data from 4 datasets against 4 baselines. We train FACT to perform action recognition with labeled RGB data, while simultaneously aligning a different set of unlabeled RGB data with synchronous IMU data. The resulting model can perform test-time inference on IMU data, showcasing cross-modal zero-shot transfer capabilities. This achievement lies at the intersection of transfer learning, multimodal representation learning, and sensor fusion and holds significant implications for the applicability of machine learning in more diverse, underexplored, modalities. Furthermore, to emphasize the importance of capturing time in sensing modalities we provide an time-continuous extension of FACT, referred to as T-FACT, that aligns modalities across extracted chunks of time, with a more powerful capability to perform zero-shot transfer in difficult scenarios. Our contributions are as follows:

- A novel motivation and setup for zero-shot cross-modal transfer learning with sensing modalities for human action recognition.
- The FACT and T-FACT infrastructures to perform zero-shot transfer to a new modality, with strong empirical results for alignment between two distinct sensing modalities.

The organization of the paper is as follows: We begin with the formulation of our setup in Section 2. We further provide an explanation of our model and methods in Section 3. Section 4 describes our results and baselines. We describe additional experiments which verify the integrity of FACT in Section 5 Then we briefly review relevant literature in Section 6. Finally, we discuss the implications and limitations of our work and conclude with Section 7.

2 Background

We investigate the creation of a robust multi-modal latent space for human action recognition, denoted as \mathcal{Z} . We refer to this latent space as \mathcal{Z} , and assume there exists a learnable mapping $h : \mathcal{Z} \rightarrow \mathcal{Y}$, where \mathcal{Y} is the label space of human actions. We further assume that there exists a learnable projection from every modality $x^{(k)} \in \mathcal{X}^{(k)}, k \in \{1 \dots M\}$ to this latent space $f^{(k)} : \mathcal{X}^{(k)} \rightarrow \mathcal{Z}$.

The critical intuition that drives our method is that for a point $z_i \in \mathcal{Z}$, any z_j "near" z_i maps to the same class as z_i , thus we can leverage the structure of \mathcal{Z} to classify any two neighboring vectors in \mathcal{Z} regardless of which modality they are generated from. In our experiments, we attempt to quantify nearby in terms of cosine similarity (and also perform some ablations with L2 distance metric).

For simplicity, we begin with 2 modalities $M = 2$ and assume n data points are split into 4 disjoint index sets $I_1 \cup I_2 \cup I_3 \cup I_4 \in \{1 \dots n\}$. Under our cross-modal transfer setting, during training the model has access to 2 of these datasets. One contains labeled data for one modality $\mathcal{D}_{HAR} = \{(\mathbf{x}_i^1, \mathbf{y}_i)\}_{i=1}^{I_1}$ and the other contains pairs of data between the modalities but these points are unlabeled: $\mathcal{D}_{Align} = \{(\mathbf{x}_i^1, \mathbf{x}_i^2)\}_{i=1}^{I_2}$. This is analogous to having an existing sensor with labeled data or a trained model, and introducing a new sensor in which data can be synchronously collected, but there is no additional annotation effort. The third and fourth sets are used for validation and testing and contain only labeled data from the second modality, i.e. $\mathcal{D}_{Val} = \{(\mathbf{x}_i^2, \mathbf{y}_i)\}_{i=1}^{I_3}$ and $\mathcal{D}_{Test} = \{(\mathbf{x}_i^2, \mathbf{y}_i)\}_{i=1}^{I_4}$.

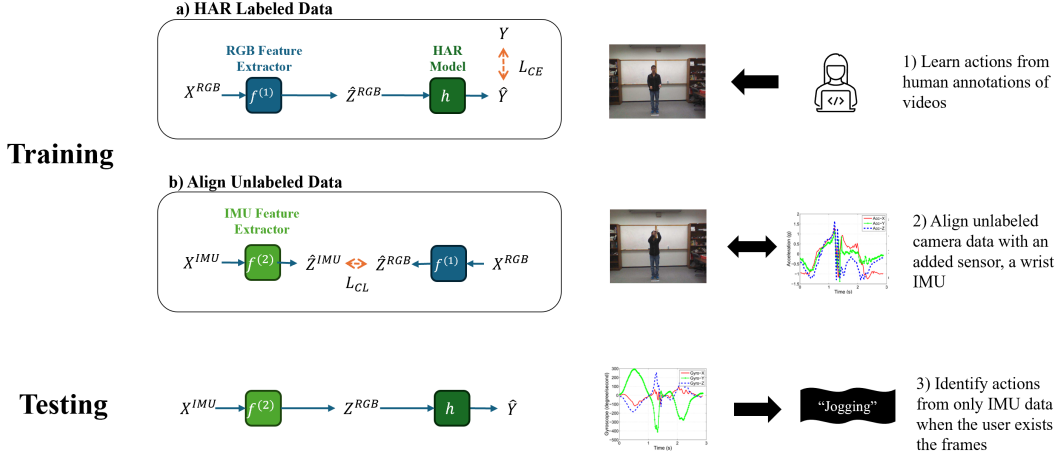


Figure 1: FACT consists of 3 modules $f^{(1)}$, $f^{(2)}$ and h described in Section 3.1. Training happens in two steps a) trains the HAR model on labeled RGB inputs and b) aligns unlabeled IMU and RGB modalities. We test the model’s ability to perform zero-shot cross-modal transfer to the IMU modality.

3 Methods

We present our Fusion and Cross-modal Transfer method to transfer knowledge to a new sensing modality without having seen labels in that modality. Given our motivation, we experiment with RGB videos as the source of labeled data $x^{(1)} = x^{(RGB)}$ and IMU data as the target data $x^{(2)} = x^{(IMU)}$.

FACT training occurs in 2 phases. Phase b) trains the HAR module on labeled camera data $x^{(1)}$ from \mathcal{D}_{HAR} and phase a) involves aligning the representations of $x^{(1)}$ with $x^{(2)}$ on \mathcal{D}_{Align} . The final results are reported on the test set where the model only has access to IMU data, \mathcal{D}_{Test} . The final results in table Table 1, show that existing works adapted to our setting heavily struggle in this zero-shot cross-modal transfer scenario. We experiment with different techniques to construct FACT and report the results in Section 5.

3.1 Model Architecture

3.1.1 FACT:

The architecture of FACT is fully modular allowing the different components to be used during the two steps of training. This also allows for scalability and interoperability of different sensing modalities, types of encoders, and output task heads. The full architecture is given in Figure 1 and the individual modules are as follows.

Video Feature Encoder $f^{(1)} : \mathcal{X}^{(1)} \rightarrow \mathcal{Z}$: This module applies a pretrained Resnet18 to every frame a video and then performs a single 3D convolution and a simple 2-layer feed forward network (FFN) with ReLU activations.

IMU Feature Encoder $f^{(2)} : \mathcal{X}^{(2)} \rightarrow \mathcal{Z}$: This module consists of a 1D CNN followed by a FFN.

HAR Task Decoder $h : \mathcal{Z} \rightarrow \mathcal{Y}$: This is a simple FFN.

3.1.2 T-FACT:

We further propose a Time-continuous FACT model that leverages the temporal information of sensing modalities when aligning and fusing their representations. In T-FACT, we remove the FFN from the feature encoders and use the output of the temporal convolutions directly. This temporal receptive field would have extracted the salient features of neighboring time steps of the data. We use each of these time steps as the a z latent vector. Then during the alignment we align each of these time vectors with the same ones from the other modality. The during phase b) when training the HAR model, we use self attention with a learned class token to predict the action. The intuition

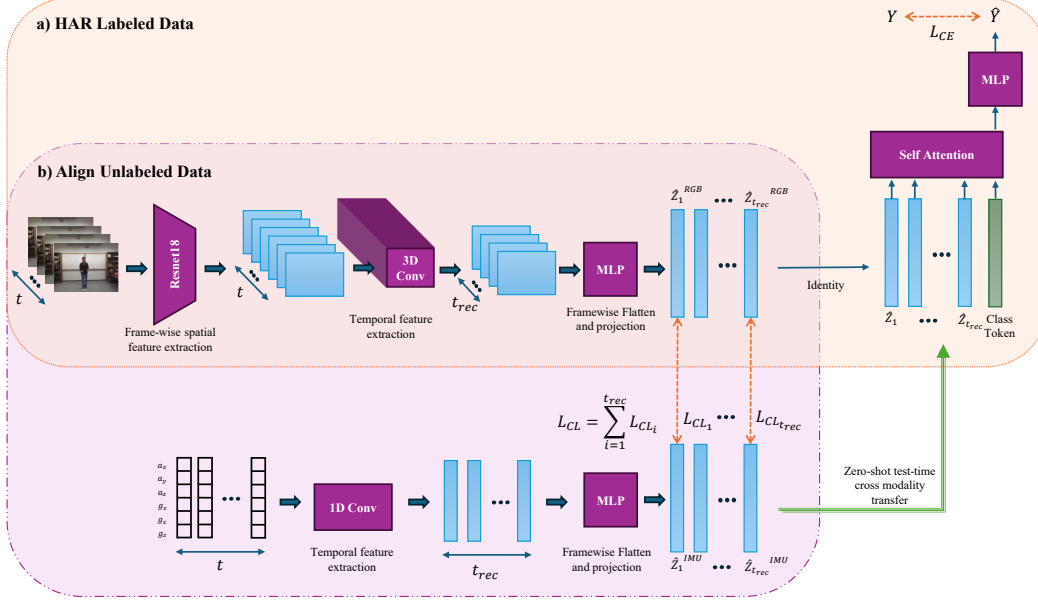


Figure 2: T-FACT is similar to FACT but aligns representations across time in the latent space and uses self attention across the time sequence to perform HAR inference. Training happens in two steps a) trains the HAR model on labeled RGB inputs and b) aligns unlabeled IMU and RGB modalities. We test the model’s ability to perform zero-shot cross-modal transfer to the IMU modality.

is that the encoder will learn which tokens over time are the most informative for the action class and predict accordingly. This is a common method to perform classification with transformers The updated modules are as follows:

Video Feature Encoder $f^{(1)} : \mathcal{X}^{(1)} \rightarrow \mathcal{Z}^{t_{rec}}$: This module applies a pretrained Resnet18 to every frame a video and then performs a single 3D convolution. The resulting output is t_{rec} vectors in \mathcal{Z} : $\hat{\mathbf{Z}}^{(1)} = (\hat{z}_1^{(1)} \dots \hat{z}_{t_{rec}}^{(1)})$.

IMU Feature Encoder $f^{(2)} : \mathcal{X}^{(2)} \rightarrow \mathcal{Z}^{t_{rec}}$: This is a 1D CNN that decreases the time dimension to t_{rec} , resulting in an output of $\hat{\mathbf{Z}}^{(2)} = (\hat{z}_1^{(2)} \dots \hat{z}_{t_{rec}}^{(2)})$.

HAR Task Decoder $h : \mathcal{Z}^{t_{rec}} \rightarrow \mathcal{Y}$: This module is like a transformer encoder that uses self-attention on an input sequence of length t_{rec} vectors appended with a learned class token. The output class token of the self attention layer is then passed through a FFN and outputs a single action label y_i .

3.2 Training and testing:

As shown in Figure 1, training iterates through two phases: training a HAR model with labeled data, and aligning the modalities’ representations using unlabeled data. For training the RGB and HAR model on \mathcal{D}_{HAR} we use the standard cross-entropy loss:

$$L_{CE} = -\frac{1}{N} \sum_{i=1}^N \sum_{j=1}^C \mathbb{1}_{i=j} \log\left(\frac{\exp \hat{y}_{i,j}}{\sum_{i=1}^M \exp \hat{y}_{i,j}}\right) \quad (1)$$

where $\hat{y}_i = h(f^{(1)}(x_i^{(1)}))$ is the output of the i th sample in the batch of N samples. $\hat{y}_{i,j}$ is the score for the j th class out of C classes.

To align different modalities in the feature space on \mathcal{D}_{Align} we use a symmetric contrastive loss formulation L_{CL} [28, 23, 11] with temperature parameter τ :

$$L_{CL} = -\frac{1}{N} \sum_{i=1}^N \log \frac{\exp(\langle \hat{z}_i^{(1)}, \hat{z}_i^{(2)} \rangle / \tau)}{\sum_{i=1}^N \exp(\langle \hat{z}_i^{(1)}, \hat{z}_i^{(2)} \rangle / \tau)}, \text{ where } \hat{z}_i^{(k)} = \frac{f^{(k)}(x_i^{(k)})}{\|f^{(k)}(x_i^{(k)})\|}, k \in \{1, 2\} \quad (2)$$

The symmetric contrastive loss will cluster representations in \mathcal{Z} by cosine similarity, which brings about the desired property of the latent space that vectors of the same class are ‘near’ each other.

Table 1: Zero-shot cross-modal transfer from the RGB to IMU sensor modalities. Imagebind on the MMACT dataset was computationally infeasible on our setup and thus is missing below.

Model	UTD-MHAD [7]	MMACT [18]	MMEA- CL [39]	CZU-MHAD [6]
Sensor Fusion (2019) [38]	5.2%	3.2 %	4.1 %	4.5 %
Student Teacher (2019) [18]	61.6%	17.1 %	9.13 %	93.9%
HAMLET (2020) [14]	4.6 %	3.2 %	4.1 %	4.5 %
ImageBind (2023) [11]	11.3 %	— %	40.1 %	4.54 %
FACT (Ours)	65.9%	33.7 %	42.7 %	77.2 %
T-FACT (Ours)	63.6%	20.6 %	47.5 %	80.3 %

\mathcal{D}_{Val} was used to search hyperparameters and perform models across experiments, on the UTD-MHAD [7] dataset. Searching was done for each baseline model individually, and testing was only done once on the best chosen model. The FACT method performed best with a learning rate of $1.5e - 3$ and a latent representation dimension of 1024. All experiments were ran on either a single 10GB NVIDIA GeForce 3080 or a single 16GB NVIDIA Quadro RTX 5000, and the exact length of the experiments varied per baseline and dataset. The model was trained in Pytorch using an Adam optimizer, the learning rate was empirically determined and the loss functions defined above.

The final reported zero shot accuracy on the \mathcal{D}_{Test} for each method is given by: $accuracy = \frac{1}{M} \sum_{i=1}^M \mathbb{1}_{\hat{y}_i = y_i}$.

4 Results

4.1 Datasets

We present results on small yet structure dataset (UTD-MHAD), one larger dataset captured in a controlled environment (CZU-MHAD), one very large dataset with various challenges (MMACT), and one egocentric camera dataset (MMEA-CL). For each of these datasets we create an approximately 40-40-10-10 percent datasplit for the \mathcal{D}_{Align} , \mathcal{D}_{HAR} , \mathcal{D}_{Val} , and \mathcal{D}_{Test} splits respectively as shown in Table 5.

UTD-MHAD Most of the development and experiments of FACT was performed on the UTD-Multi-modal Human Action Dataset (UTD-MHAD) [7]. This dataset consists of roughly 861 sequences of RGB, skeletal, depth and an inertial sensor, with 27 different labeled action classes performed by 8 subjects 4 times. The inertial sensor provided 3-axis acceleration and 3-axis gyroscopic information, and all 6 channels were used for in our model as the IMU input. Given our motivation, we only use the video and inertial data; however, FACT can easily be extended to multiple modalities.

CZU-MHAD The Changzhou MHAD [6] dataset provides about 1,170 sequences and includes depth information from a Kinect camera synchronized with 10 IMU sensors, each 6 channels, in a very controlled setting with a user directly facing the camera. We concatenate the IMU data to provide a 60-channel input as the IMU modality and use depth as the input modality. Given the controlled environment and dense IMU streams, the models performed the best on this dataset.

MMACT The MMACT dataset [18] is a large scale dataset containing about 1,900 sequences of 35 action classes from 40 subjects on 7 modalities. This data is challenging because it provides data from 5 different scenes, including sitting a desk, or performing an action that is partially occluded by an object. Furthermore, the data was collected with the user facing random angles at random times. The dataset contains 4 different cameras at 4 corners of the room, and it measures acceleration on the user’s watch and acceleration, gyroscope and orientation data from a user’s phone in their pocket. We only use the cross-view camera 1 data, and again we concatenate the 4 3-axis inertial sensors into one 12 channel IMU modality.

MMEA-CL The multimodal egocentric activity recognition dataset for continual learning (MMEA-CL) is a recent dataset motivated by learning strong visual-IMU based representations that can be used for continual learning. It provides about 6,4000 samples of synchronized first-person video clips and 6-channel accelerometer and gyroscope data from a wrist worn IMU. The dataset’s labels features realistic daily actions in the wild, as opposed to recorded sequences in a lab. Due to issues with the data and technical constraints, we downsize the data proportionally and use about 1,000 samples. Nonetheless, FACT’s superior performance shows how this method can generalize to a different camera view, and different types of activities.

4.2 Baselines

Many works deal with robustness to missing sensor data during training or testing, however, few works deal with zero-labeled training data from one modality. As a result, constructing baselines was tricky and most methods had to be modified or adopted to fit our approach.

4.2.1 Student Teacher Baseline

Various student teacher models have been proposed [18, 35, 3]. However, these models often assume the availability of student-teacher labeled modality pairs during training to distill knowledge from the teacher to the student when updating the corresponding losses. Thus most of these architectures are not directly applicable. Nonetheless, we borrow the basic concept of a teacher modality distilling knowledge to the student modality through psuedo labels, most similar to [32].

We denote the teacher network as $g^{(t)} : \mathcal{X}^{(1)} \rightarrow \mathcal{Y}$ and the student network as $g^{(s)} : \mathcal{X}^{(2)} \rightarrow \mathcal{Y}$. Our designated student-teacher baseline uses \mathcal{D}_{HAR} to train $g^{(t)}$ on the RGB data. Next, in order to train $g^{(s)}$ on \mathcal{D}_{Align} , we first use $g^{(t)}(x_1^{(1)}) = \hat{y}_1$ to generate psuedo-labels for every datapoint $i \in I_2$. Then we use the augmented dataset $\hat{\mathcal{D}}_{Align} = \{(\mathbf{x}_i^1, \mathbf{x}_i^2, \hat{y}_i)\}_{i=1}^{I_2}$ to train $g^{(s)}$. We note that $g^{(t)}$ and $g^{(s)}$ have similar architectures to $h(f^{(1)}(\cdot))$ and $h(f^{(2)}(\cdot))$, respectively for a fair performance comparison.

This student teacher baseline presents a strong solution for our setup, and gives a competitive performance in Table 1. However, the only method it outperforms FACT was in the relatively easy CZU-MHAD dataset. One drawback, with this model is that it requires labeled data from both modalities to improve it’s performance, whereas FACT can use unlabeled data to learn some correlation between modalities in \mathcal{Z} . This representation space can be used for other purposes as well, such as dynamically adding modalities or task specific heads.

4.2.2 Sensor Fusion Baselines

Many IMU-RGB based sensor fusion models have the ability to train on partially available or corrupted data and are robust to missing modalities during inference [15, 14]. No works have attempted the extreme case where one modality is completely unlabeled during training. Existing ensor fusion methods can be adapted to our setup using a psuedo-labeling technique, similar to the student-teacher model above. The difference here is that the model learns a joint distribution between the two modalities so hopefully it may be able to learn some correlation between the models. Nonetheless, we show that these methods cannot generalize to the scenario where there is zero-labeled training data for one modality.

Let $g(\cdot, \cdot) : (\mathcal{X}^{(1)}, \mathcal{X}^{(2)}) \rightarrow \mathcal{Y}$. Our approach uses \mathcal{D}_{HAR} , to train by passing in zeros for one modality, e.g. we train $g(\cdot, \mathbf{0}) : \mathcal{X}^{(1)} \rightarrow \mathcal{Y}$. Then, with \mathcal{D}_{Align} we use $g(\cdot, \mathbf{0})$ to generated psuedo-labels and then train $g(\mathbf{0}, \cdot)$ with those labels.

We reproduced the conventional sensor fusion models (early, feature, and late) from [38] and indicate the performance of the top model on 1. We further reproduce a self-attention based sensor fusion appraoch (HAMLET [14]) and tested it on our setup. We selected these model due to their state-of-the-art performance on the UTD-MHAD dataset, making them ideal benchmarks for comparison with our model.

4.2.3 Contrastive Learning Baseline

ImageBind [11] learns encoders for 6 modalities, (Images/Videos, Text, Audio, Depth, Thermal and IMU) by performing CLIP’s training method [28] between each of those encoders and the Image/Video encoder. It was well tested for image, text and audio based alignment, retrieval and latent space generation tasks, however was not well test with IMU data and not used for specific tasks, such as HAR. In addition, one fundamental difference between Imagebind and FACT is that Imagebind constructs a latent space amongst the sensing modalities and text and aligns between them. We hypothesize that this is vector space is more difficult and unnecessary to construct, for human action recognitoin using sensing modalities. The text modality, although sequential in nature, does not have a time dimension, thus it cannot leverage correlations between modalities in time like T-FACT.

Let’s denote the video, IMU and text encoders as $g^{(1)} : \mathcal{X}^{(1)} \rightarrow \mathcal{Z}$, $g^{(2)} : \mathcal{X}^{(2)} \rightarrow \mathcal{Z}$, and $g^{(3)} : \mathcal{X}^{(3)} \rightarrow \mathcal{Z}$ respectively. We perform two conventional task-specific adaptations for CLIP models. First, we attempt zero-shot transfer, in which we pass all the action labels through the text encoder. For a dataset with C classes, we have $\hat{\mathcal{Z}}^{(3)} = (\hat{z}_1^{(3)} \dots \hat{z}_C^{(3)})$. Finally, for a given IMU sample $(x_i^{(2)}, y_i) \in \mathcal{D}_{Test}$, we pass $x_i^{(2)}$ through the IMU encoder $g^{(2)}$ and retrieve $\hat{z}^{(2)}$. Finally, we classify the point by looking at which points gives the highest cosine similarity score in the latent space, e.g. $\hat{y}_i = \underset{j}{argmax} \frac{\langle x_i^{(2)}, \hat{z}_j^{(3)} \rangle}{\| \langle x_i^{(2)}, \hat{z}_j^{(3)} \rangle \|}$.

Table 2: Extending the test set of UTD-MHAD to include both modalities, FACT can maintain performance on the RGB data, only use IMU data, or fuse the data depending on which modalities are given during inference(Section 5.2)

Model	1. RGB	2. IMU	3. Fusion
Sensor Fusion	45%	5.2%	5.2%
Student Teacher	83.7%	61.6%	80.2%
ImageBind	40%	3.4%	33%
FACT (Ours)	90.9%	65.9%	84.1%
T-FACT (Ours)	93.2%	63.6%	88.6%

Table 3: Extending the test set of CZU-MHAD to include both modalities, we notice Fusion performs better than RGB

Model	1. RGB	2. IMU	3. Fusion
Sensor Fusion	4.6%	4.6%	4.6%
Student Teacher	96.2%	77.2%	95.6%
FACT (Ours)	90.9%	65.9%	84.1%
T-FACT (Ours)	86.4%	75.8%	88.6%

Table 4: Different methods to Train FACT and their results on zero-shot IMU data

Experiment	Test Accuracy on IMU
1) Align First	65.9%
2) HAR First	36.36%
3) Interspersed Training	13.64%
4) Combined Loss	63.64%

Given that ImageBind is a large model trained on massive corpuses of data it becomes impractical to train the model from scratch on our smaller datasets collected from wearables and edge devices. Instead, we fine-tuned the ImageBind model using a linear projection head on the encoders, that can then be trained for a specific task. The results of this method are depicted in Table 1.

The results show a poor generalization of Imagebind to most experiments on our setup, and we hypothesize a few reasons. Firstly, ImageBind is a large model and may either overfit to small datasets, or not have enough training examples to learn strong enough representations. Second, ImageBind was pre-trained on Ego4D and Aria which contain egocentric videos to align noisy captions with the IMU data, whereas our datasets had fixed labels and were mostly 3rd person perspective. In fact ImageBind performed the best on the one egocentric dataset we used, MMEA-CL[39]. Lastly, Imagebind was trained on a IMU sequences of 10s length sampled at a much higher frequency, thus we zero-padded or upsampled the IMU data to fit into ImageBind’s IMU encoder, and the sparse or repetitive signal may have been too weak for ImageBind’s encoder to accurately interpret the data.

5 Additional Experiments and Ablations

FACT is modular and scalable and well suited for time series sensor data. Here we perform ablations and experiments to show how our design is uniquely structured to perform cross-modal transfer for zero-shot transfer well. We conduct two primary sets of experiments: one investigates various training mechanisms of FACT, and the other examines the deployment of the model in different testing scenarios.

5.1 Training Experiments

We conducted four primary experiments to identify the optimal training method for the FACT infrastructure, using the UTD-MHAD dataset. FACT employs two distinct losses, each corresponding to a different part of the training process as illustrated in Figure 1. We experimented with various ways to combine these two losses and determined the most effective approach, as shown in Table 4.

1) Align First: The first experiment first aligns the representations generated by the RGB and IMU encoders, $f^{(1)}$ and $f^{(2)}$ RGB on \mathcal{D}_{Align} (phase a) of training). Then the weights for both encoders are frozen and the HAR module h is trained on the latent representation $\hat{z}^{(1)}$ generated from the RGB encoder.

2) HAR First: In this method, we first perform phase b) and the RGB HAR model completely with the \mathcal{D}_{Align} split of data. Then we freeze the encoder $f^{(1)}$ and align the modalities with the \mathcal{D}_{HAR} split of data (phase a).

3) Interspersed Training: Here the model intermittently learns from \mathcal{D}_{Align} and \mathcal{D}_{HAR} . The model learns an epoch from b) and updates it’s weights to train the RGB HAR model, then learns an epoch from a) and updates it’s weights to align the encoders. The model continues to iterate between the two losses. We also experimented with training within each batch but using different losses and optimizers, but this yielded instability in the training.

4) Combined Loss: This method trains both a) and b) but within the same loss iteration. The loss from a) on a batch of data from \mathcal{D}_{Align} is added to the loss from b) on a batch of data from \mathcal{D}_{HAR} and the total loss is then

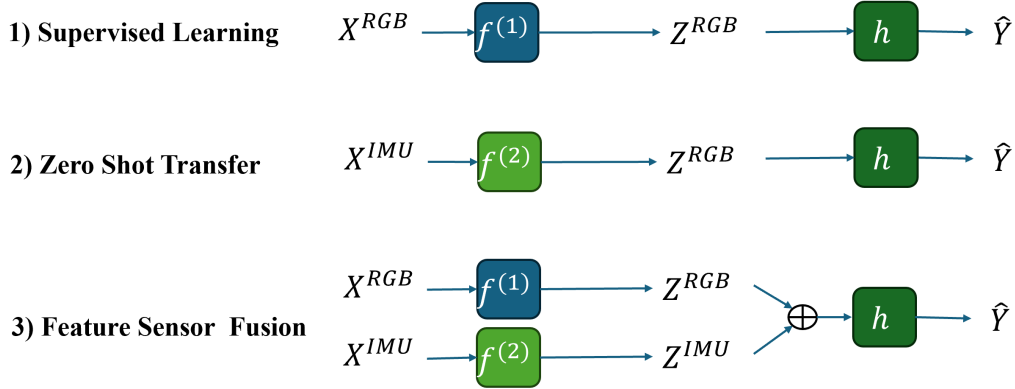


Figure 3: We can perform inference with the model with any subset of it’s original input modalities.

used to update the weights of the model.

$$L_{Total} = L_{CE} + L_{CL} \quad (3)$$

The results in Table 4 indicate that the first method of aligning the modalities yields the best results. We hypothesize that in experiment 2, training the HAR model first, yields a latent space tailored to capturing the best features distinguishing action classes from RGB data, which is not directly applicable to IMU data. As mentioned above the loss graphs of experiment 3 indicate instability in training. Experiment 4, performed similarly well to 1 which could be due to the idea that one loss acts as a regularizer for the other one pushing the latent space \mathcal{Z} to the ideal space for cross-modal transfer we discussed in Section 2. The results reported in Table 1 use method 1.

5.2 Testing Experiments

We have shown that the FACT performs well on a new modality, however, the question remains whether it can still retain performance on the original modality it was trained on. Furthermore, if it is given multiple modalities during inference, can it leverage information from all of them? Through FACT, for any data sample i given for inference, regardless of whether the sample contains data from $\mathcal{X}^{(1)}$, $\mathcal{X}^{(2)}$ or both $(\mathcal{X}^{(1)}, \mathcal{X}^{(2)})$, we can estimate the latent vector $\hat{z}_i \in \mathcal{Z}$ and thus predict the action using the HAR module, $\hat{y} = h(\hat{z}_i)$

1. RGB (Supervised Learning) The typical supervised machine learning paradigm tests the model on different samples of the same distribution. In our case, this is testing FACT on RGB data. Thus the estimated latent vector is given by $f^{(1)}(x_i^{(1)}) = \hat{z}_i$.

2. IMU (Zero-Shot Transfer) The cross-modal zero-shot transfer method is the main result of this paper and described above in Section 3. Here the estimated latent vector is given by $f^{(2)}(x_i^{(2)}) = \hat{z}_i$.

3. Fusion (Sensor Fusion) When both modalities are present, the model estimates the latent vector \hat{z}_i from the outputs of modality-specific encoders assuming each estimate is equally as good as the other. $\hat{z}_i = \mathbb{E}[z_i | x_i^{(1)}, x_i^{(2)}] = E[z_i | \hat{z}_i^{(1)}, \hat{z}_i^{(2)}] = \frac{\hat{z}_i^{(1)} + \hat{z}_i^{(2)}}{2}$. Thus, for sensor fusion we average the outputs of each of the encoders. We show the results in 1 and 2.

6 Related Works

6.1 Sensor Fusion

Cross-modal transfer learning is a method to transfer knowledge from a modality with abundant training data to one with limited data [24]. Domain adaptation can be seen as a subset of cross-modal transfer. Domain adaptation allows a machine learning model trained in one domain to efficiently adapt to another related domain for the same output task with fewer data labels [25, 8]. Given this focus on scarcely labeled domains, adaptation is often performed through unsupervised [5] or semi-supervised [1] methods. In terms of human activity recognition, different data domains can imply adapting between different sensor inputs [2], different positions of wearables on the human body [34, 5, 27], different users [13, 10] or IMU device type [17, 41, 4]. In the context of this cross-modal learning our work may be considered domain adaptation involving different sensor inputs.

IMU Virtualization: To overcome the difficulties associated with limited IMU data, many recent works have leveraged the ability to simulate IMU data from videos such as IMUTube [19] or ChromoSim [12]. This allows them to train an IMU model from camera data and perform zero-shot classification on IMU data with a model that has never seen real IMU data. However, these models are time and data-intensive and cannot easily be extended to other modalities.

Contrastive Learning Methods: Contrastive learning-based multimodal models such as ImageBind [11] or IMU2CLIP [23] are relatively easy to extend to new modalities, however, they fail to fuse the sensor modalities when present and are designed for cross-modal retrieval or generation and perform poorly on specific tasks such as human action recognition.

Cross-Modal Knowledge Distillation Knowledge distillation methods typically use an extra auxiliary modality during training to increase single modal performance during testing, however, they assume labeled training data from both modalities during training [40, 18, 35, 3]. Notably, [32] attempts to perform without knowledge distillation without labels for one modality using a student-teacher framework which FACT can out-perform. Furthermore, they test transferring across visual modalities which is likely more correlated than visual and inertial modalities.

7 Conclusion

Limitations: Our experiments were run in a very controlled predefined environment and SF-CMT is a research prototype. Future extensions of this work may want to consider the more realistic application of continuous HAR, where the system also must localize the action temporally and spatially before being able to recognize it. We anticipate that T-FACT would work well in this instance. Another relevant extension would be to increase the generalizability of the model, by adding a dimension of inductive transfer, i.e. transfer across output distributions. This means creating a model that could transfer knowledge across different input modalities and different output tasks. Currently, the method is not well tested with more than two modalities, and thus the proposed fusion mechanism in Section 5.2 is under-explored. Even with two modalities, the model performs better using just RGB data than Fusing both; however, we posit that there may be some sort of weighted fusion mechanism that can leverage the IMU data to improve performance with both modalities.

Conclusion: Achieving a good performance with such a compact network demonstrates how this work is essential to the development of cross-modal transfer learning. FACT has a unique theoretical intuition, guiding its design to construct a joint latent space between modalities, that can leverage correlations between them while performing human action recognition. This framework allows the model to train with zero labels for one modality and still performance inference with that modality alone. Our result has shown promising empirical results on the novel setting of zero shot cross-modal transfer between sensor representations. Especially for biometric or smart IoT applications where the physical form factor is constrained, training data is scarce, and FACT is a viable method for cross-modal transfer.

References

- [1] Sungtae An, Alessio Medda, Michael N Sawka, Clayton J Hutto, Mindy L Millard-Stafford, Scott Appling, Kristine LS Richardson, and Omer T Inan. Adaptnet: human activity recognition via bilateral domain adaptation using semi-supervised deep translation networks. *IEEE Sensors Journal*, 21(18):20398–20411, 2021.
- [2] Sejal Bhalla, Mayank Goel, and Rushil Khurana. Imu2doppler: Cross-modal domain adaptation for doppler-based activity recognition using imu data. *Proceedings of the ACM on Interactive, Mobile, Wearable and Ubiquitous Technologies*, 5(4):1–20, 2021.
- [3] XB Bruce, Yan Liu, and Keith CC Chan. Multimodal fusion via teacher-student network for indoor action recognition. In *Proceedings of the AAAI Conference on Artificial Intelligence*, volume 35, pages 3199–3207, 2021.
- [4] Avijoy Chakma, Abu Zaher Md Faridee, Md Abdullah Al Hafiz Khan, and Nirmalya Roy. Activity recognition in wearables using adversarial multi-source domain adaptation. *Smart Health*, 19:100174, 2021.
- [5] Youngjae Chang, Akhil Mathur, Anton Isopoussu, Juneha Song, and Fahim Kawsar. A systematic study of unsupervised domain adaptation for robust human-activity recognition. *Proceedings of the ACM on Interactive, Mobile, Wearable and Ubiquitous Technologies*, 4(1):1–30, 2020.
- [6] Xin Chao, Zhenjie Hou, and Yujian Mo. Czu-mhad: A multimodal dataset for human action recognition utilizing a depth camera and 10 wearable inertial sensors. *IEEE Sensors Journal*, 22(7):7034–7042, 2022.

- [7] Chen Chen, Roozbeh Jafari, and Nasser Kehtarnavaz. Utd-mhad: A multimodal dataset for human action recognition utilizing a depth camera and a wearable inertial sensor. In *2015 IEEE International conference on image processing (ICIP)*, pages 168–172. IEEE, 2015.
- [8] Abolfazl Farahani, Sahar Voghoei, Khaled Rasheed, and Hamid R Arabnia. A brief review of domain adaptation. *Advances in data science and information engineering: proceedings from ICDATA 2020 and IKE 2020*, pages 877–894, 2021.
- [9] Yao Feng, Jing Lin, Sai Kumar Dwivedi, Yu Sun, Priyanka Patel, and Michael J Black. Posegpt: Chatting about 3d human pose. *arXiv preprint arXiv:2311.18836*, 2023.
- [10] Zhongzheng Fu, Xinrun He, Enkai Wang, Jun Huo, Jian Huang, and Dongrui Wu. Personalized human activity recognition based on integrated wearable sensor and transfer learning. *Sensors*, 21(3):885, 2021.
- [11] Rohit Girdhar, Alaeldin El-Nouby, Zhuang Liu, Mannat Singh, Kalyan Vasudev Alwala, Armand Joulin, and Ishan Misra. Imagebind: One embedding space to bind them all. In *Proceedings of the IEEE/CVF Conference on Computer Vision and Pattern Recognition*, pages 15180–15190, 2023.
- [12] Yujiao Hao, Xijian Lou, Boyu Wang, and Rong Zheng. Cromosim: A deep learning-based cross-modality inertial measurement simulator. *IEEE Transactions on Mobile Computing*, 2022.
- [13] Rong Hu, Ling Chen, Shenghuan Miao, and Xing Tang. Swl-adapt: An unsupervised domain adaptation model with sample weight learning for cross-user wearable human activity recognition. In *Proceedings of the AAAI Conference on artificial intelligence*, volume 37, pages 6012–6020, 2023.
- [14] Md Mofijul Islam and Tariq Iqbal. Hamlet: A hierarchical multimodal attention-based human activity recognition algorithm. In *2020 IEEE/RSJ International Conference on Intelligent Robots and Systems (IROS)*, pages 10285–10292. IEEE, 2020.
- [15] Md Mofijul Islam, Mohammad Samin Yasar, and Tariq Iqbal. Maven: A memory augmented recurrent approach for multimodal fusion. *IEEE Transactions on Multimedia*, 2022.
- [16] Shuiwang Ji, Wei Xu, Ming Yang, and Kai Yu. 3d convolutional neural networks for human action recognition. *IEEE transactions on pattern analysis and machine intelligence*, 35(1):221–231, 2012.
- [17] Md Abdullah Al Hafiz Khan, Nirmalya Roy, and Archan Misra. Scaling human activity recognition via deep learning-based domain adaptation. In *2018 IEEE international conference on pervasive computing and communications (PerCom)*, pages 1–9. IEEE, 2018.
- [18] Quan Kong, Ziming Wu, Ziwei Deng, Martin Klinkigt, Bin Tong, and Tomokazu Murakami. Mmact: A large-scale dataset for cross modal human action understanding. In *Proceedings of the IEEE/CVF International Conference on Computer Vision*, pages 8658–8667, 2019.
- [19] Hyeokhyen Kwon, Catherine Tong, Harish Haresamudram, Yan Gao, Gregory D Abowd, Nicholas D Lane, and Thomas Ploetz. Imutube: Automatic extraction of virtual on-body accelerometry from video for human activity recognition. *Proceedings of the ACM on Interactive, Mobile, Wearable and Ubiquitous Technologies*, 4(3):1–29, 2020.
- [20] Ziyi Lin, Shijie Geng, Renrui Zhang, Peng Gao, Gerard de Melo, Xiaogang Wang, Jifeng Dai, Yu Qiao, and Hongsheng Li. Frozen clip models are efficient video learners. In *Computer Vision–ECCV 2022: 17th European Conference, Tel Aviv, Israel, October 23–27, 2022, Proceedings, Part XXXV*, pages 388–404. Springer, 2022.
- [21] Sharmin Majumder and Nasser Kehtarnavaz. Vision and inertial sensing fusion for human action recognition: A review. *IEEE Sensors Journal*, 21(3):2454–2467, 2020.
- [22] Vimal Mollyn, Riku Arakawa, Mayank Goel, Chris Harrison, and Karan Ahuja. Imuposer: Full-body pose estimation using imus in phones, watches, and earbuds. In *Proceedings of the 2023 CHI Conference on Human Factors in Computing Systems*, pages 1–12, 2023.
- [23] Seungwhan Moon, Andrea Madotto, Zhaojiang Lin, Alireza Dirafzoon, Aparajita Saraf, Amy Bearman, and Babak Damavandi. Imu2clip: Multimodal contrastive learning for imu motion sensors from egocentric videos and text. *arXiv preprint arXiv:2210.14395*, 2022.
- [24] Shuteng Niu, Yongxin Liu, Jian Wang, and Houbing Song. A decade survey of transfer learning (2010–2020). *IEEE Transactions on Artificial Intelligence*, 1(2):151–166, 2020.
- [25] Sinno Jialin Pan and Qiang Yang. A survey on transfer learning. *IEEE Transactions on knowledge and data engineering*, 22(10):1345–1359, 2009.

- [26] AJ Piergiovanni, Weicheng Kuo, and Anelia Angelova. Rethinking video vits: Sparse video tubes for joint image and video learning. In *Proceedings of the IEEE/CVF Conference on Computer Vision and Pattern Recognition*, pages 2214–2224, 2023.
- [27] Aria Ghora Prabono, Bernardo Nugroho Yahya, and Seok-Lyong Lee. Hybrid domain adaptation with deep network architecture for end-to-end cross-domain human activity recognition. *Computers & Industrial Engineering*, 151:106953, 2021.
- [28] Alec Radford, Jong Wook Kim, Chris Hallacy, Aditya Ramesh, Gabriel Goh, Sandhini Agarwal, Girish Sastry, Amanda Askell, Pamela Mishkin, Jack Clark, et al. Learning transferable visual models from natural language supervision. In *International Conference on Machine Learning*, pages 8748–8763. PMLR, 2021.
- [29] Dhanesh Ramachandram and Graham W Taylor. Deep multimodal learning: A survey on recent advances and trends. *IEEE signal processing magazine*, 34(6):96–108, 2017.
- [30] Rajeev Sharma, Vladimir I Pavlovic, and Thomas S Huang. Toward multimodal human-computer interface. *Proceedings of the IEEE*, 86(5):853–869, 1998.
- [31] Karen Simonyan and Andrew Zisserman. Two-stream convolutional networks for action recognition in videos. *Advances in neural information processing systems*, 27, 2014.
- [32] Fida Mohammad Thoker and Juergen Gall. Cross-modal knowledge distillation for action recognition. In *2019 IEEE International Conference on Image Processing (ICIP)*, pages 6–10. IEEE, 2019.
- [33] Zhan Tong, Yibing Song, Jue Wang, and Limin Wang. Videomae: Masked autoencoders are data-efficient learners for self-supervised video pre-training. *Advances in neural information processing systems*, 35: 10078–10093, 2022.
- [34] Jindong Wang, Vincent W Zheng, Yiqiang Chen, and Meiyu Huang. Deep transfer learning for cross-domain activity recognition. In *proceedings of the 3rd International Conference on Crowd Science and Engineering*, pages 1–8, 2018.
- [35] Qi Wang, Liang Zhan, Paul Thompson, and Jiayu Zhou. Multimodal learning with incomplete modalities by knowledge distillation. In *Proceedings of the 26th ACM SIGKDD International Conference on Knowledge Discovery & Data Mining*, pages 1828–1838, 2020.
- [36] Rui Wang, Dongdong Chen, Zuxuan Wu, Yinpeng Chen, Xiyang Dai, Mengchen Liu, Lu Yuan, and Yu-Gang Jiang. Masked video distillation: Rethinking masked feature modeling for self-supervised video representation learning. In *Proceedings of the IEEE/CVF Conference on Computer Vision and Pattern Recognition*, pages 6312–6322, 2023.
- [37] Yi Wang, Kunchang Li, Yizhuo Li, Yinan He, Bingkun Huang, Zhiyu Zhao, Hongjie Zhang, Jilan Xu, Yi Liu, Zun Wang, et al. Internvideo: General video foundation models via generative and discriminative learning. *arXiv preprint arXiv:2212.03191*, 2022.
- [38] Haoran Wei, Roozbeh Jafari, and Nasser Kehtarnavaz. Fusion of video and inertial sensing for deep learning-based human action recognition. *Sensors*, 19(17):3680, 2019.
- [39] Linfeng Xu, Qingbo Wu, Lili Pan, Fanman Meng, Hongliang Li, Chiyuan He, Hanxin Wang, Shaoxu Cheng, and Yu Dai. Towards continual egocentric activity recognition: A multi-modal egocentric activity dataset for continual learning. *IEEE Transactions on Multimedia*, 2023.
- [40] Zihui Xue, Zhengqi Gao, Sucheng Ren, and Hang Zhao. The modality focusing hypothesis: Towards understanding crossmodal knowledge distillation. *arXiv preprint arXiv:2206.06487*, 2022.
- [41] Zhijun Zhou, Yingtian Zhang, Xiaojing Yu, Panlong Yang, Xiang-Yang Li, Jing Zhao, and Hao Zhou. Xhar: Deep domain adaptation for human activity recognition with smart devices. In *2020 17th Annual IEEE International Conference on Sensing, Communication, and Networking (SECON)*, pages 1–9. IEEE, 2020.

A Appendix / supplemental material

A.1 UTD-MHAD Dataset

The UTD-MHAD dataset has no predefined splits and benchmarks, and little to no works have open sourced their code on it. As such, to ensure we were using the data correctly implemented a few sensor fusion models and compared to state-of-the-art reported methods and showed similar performance results. The results are given in Table 6 These experiments provide a standard of comparison for our results with other methods on the UTD-MHAD dataset, and these models are available in the code for this paper.

Table 5: Data Splits

Split Name	% of Data	Provided Data
Train a)	40%	(X^{RGB}, Y)
Train b)	40%	(X^{RGB}, X^{IMU})
Validation	10%	(X^{RGB}, X^{IMU}, Y)
Test	10%	(X^{RGB}, X^{IMU}, Y)

Table 6: SOTA Sensor Fusion Performance on UTD-MHAD

REPORTED MODELS	ACCURACY
HAMLET [14]	95.12%
WEI ET AL. [38]	95.6%
REPRODUCED FROM [38]	ACCURACY
EARLY FUSION	86.71%
FEATURE FUSION	95.60%
LATE FUSION	94.22%

A.2 Baselines

A.2.1 HAMLET

Given that there is no open source implementation for the HAMLET attention based sensor fusion method [14], we reproduce it from scratch. We follow a very similar architecture; however, extract spatio-temporal results using 3D convolution in the video as opposed to an LSTM and show similar results on the standard sensor fusion problem.

A.2.2 Sensor Fusion

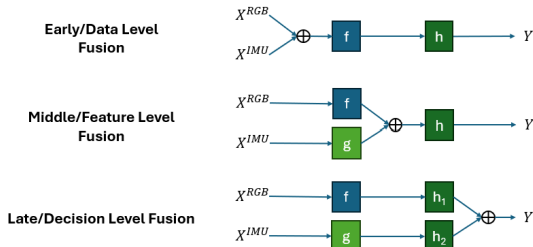


Figure 4: Types of Sensor Fusion

Sensor fusion is often broken down into the following 3 methods based on where the data are combined [29, 21, 30], also shown in Figure 4: 1) Early or data-level fusion combines the raw sensor outputs before any processing. 2) Middle/intermediate or feature-level fusion combines each sensor modality after some preprocessing or feature extraction. 3) Late or decision-level fusion combines the raw output, essentially ensembling separate models.